Original Article

DOI: 10.5582/ddt.2024.01035

# Duzhong Fang ameliorates cognitive impairment of Parkinsonian mice by suppressing neuronal apoptotic pathway

**Qian Shen[1,§], Ruiting Liu[1,§], Yu Wang[1], Pengwei Zhuang[2,3], Weihong Yang[1,*], Hong Guo[1,*]**

[1] State Key Laboratory of Component-based Chinese Medicine, Tianjin University of Traditional Chinese Medicine, Tianjin, China;
[2] Haihe Laboratory of Modern Chinese Medicine, Tianjin, China;
[3] First Teaching Hospital of Tianjin University of Traditional Chinese Medicine, Tianjin, China.

**SUMMARY** Parkinson's disease (PD) is a complex multisystem neurodegenerative disease, and cognitive impairment is a common symptom in the trajectory of PD. Duzhong Fang (DZF) consists of *Eucommia ulmoides*, *Dendrobium*, *Rehmanniae Radix*, and *Dried Ginger*. Our previous study showed that DZF improves motor deficits in mice. However, whether DZF can ameliorate cognitive impairment in PD has not been reported. In this study, we established mice models of PD induced by rotenone and examined the effect of DZF on cognitive impairment in Parkinson's disease (PD-CI). The results confirmed that DZF treatment not only significantly improved the motor deficits in PD mice and decreased the loss of dopaminergic neurons, but also had significant effects in improving cognitive impairment. We further integrate serum metabolome and network pharmacology to explore the mechanisms by which DZF improves PD-CI. The results revealed that DZF can treat PD-CI by regulating sphingolipid metabolism to inhibit neuronal apoptotic pathway. In conclusion, preliminary studies confirmed that DZF contributes to the improvement of cognitive ability in PD, and our results provide a potential drug for the clinical treatment of PD and a theoretical foundation for DZF in clinical application.

***Keywords*** Cognitive impairment, Parkinson's disease, Duzhong Fang, sphingolipid metabolism, apoptosis

## 1. Introduction

Cognitive impairment is one of the most common non-motor symptoms of Parkinson's disease (PD) (*1*). At present, in PD patients with a course of 10 years or more, the cumulative prevalence of cognitive impairment in Parkinson's disease (PD-CI) is 75-90% (*2*). With the increasing life expectancy of PD patients, PD-CI is set to become even more prevalent in the future (*3*). Cognitive impairment greatly worsens life quality in patients, as well as increases caregiver burden and health care costs. However, at present there is no effective drug for the treatment of PD-CI (*4*). For PD-CI, drugs for Alzheimer's disease (AD) are mostly clinically selected. Nevertheless, due to the pathogenesis being different, the treatment effects were not obvious. Therefore, investigating potential drugs for cognitive restoration, and treatment of PD-CI earlier is vital to improved social functioning and quality of life for these patients.

Duzhong Fang (DZF) comes from the Handbook of Prescriptions for Emergencies, which consists of *Eucommia ulmoides*, *Dendrobium*, *Rehmanniae Radix*, and *Dried Ginger*. Our previous study demonstrated that DZF can improve movement disorders and reduce the loss of dopaminergic neurons in PD mice (*5*). Nevertheless, its effect on PD-CI has not been reported. Previous studies have found that *Eucommia ulmoides*, *Dendrobium,* and *Radix rehmanniae* can improve cognitive impairment (*6-8*). It is reasonable to speculate that DZF may not only improve movement disorders but also ameliorate cognitive impairment in PD patients.

In this study, rotenone induced PD model was used to examine the beneficial effects of DZF against PD-CI. Then, the underlying mechanisms of how DZF contributes to the cognitive improvement in PD mice were further explored *via* network pharmacology, metabolomics, immunohistochemical and biochemical analysis. Our data suggested that DZF improved cognitive ability by inhibiting neuronal apoptotic pathway. Figure 1 below illustrates the process and the key findings of the study.

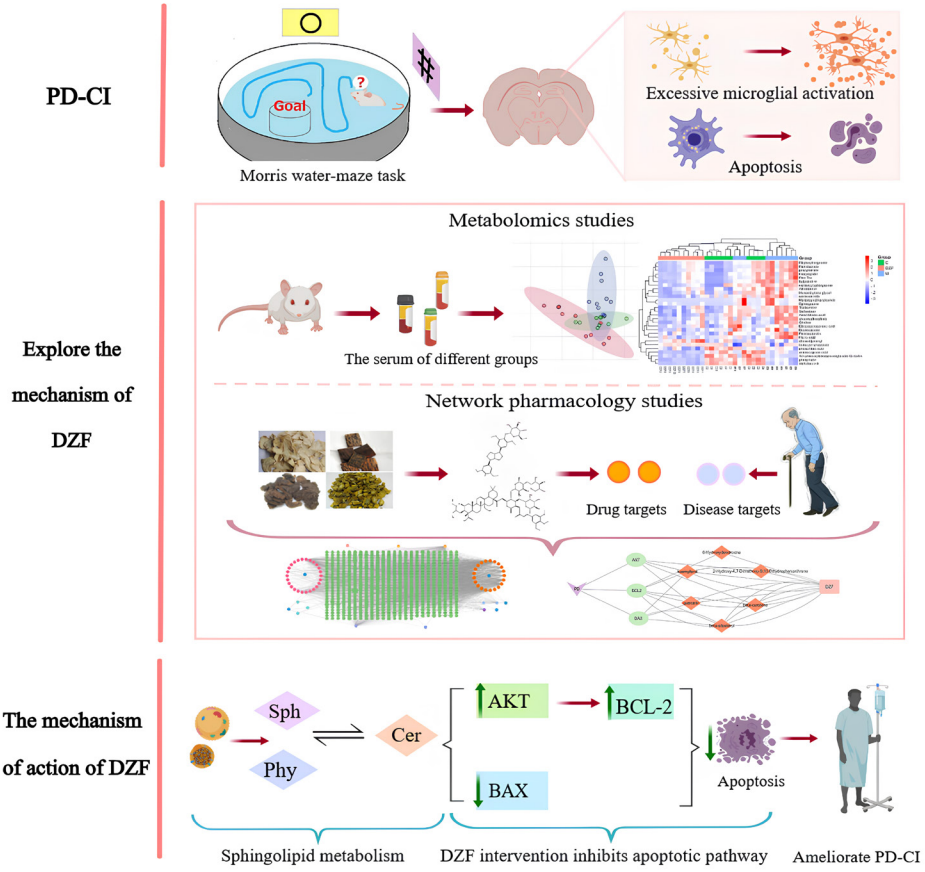


**Figure 1. The process and the key findings of the study.**

## 2. Materials and Methods

### 2.1. Reagents

*Eucommia ulmoides*, *Dendrobium*, *Rehmanniae Radix*, and *Dried Ginger* were obtained from Beijing Tongrentang (Beijing, China). Rotenone was purchased from Sigma Chemical Co (St. Louis, MO, USA). 4% paraformaldehyde was purchased from Coolaber (Beijing, China). Triton-100 X was supplied by Beijing Suolaibao Technology Co. Ltd. (Beijing, China). Tyrosinehydroxylase (TH)/ Ionized c alcium bindingadaptor molecule-1 (Iba-1) / Neuronal nuclear antigen (Neu-N) rabbit antibodies were supplied from Abcom (Cambridge, MA, USA). Radioimmunoprecipitation assay buffer (RIPA) and protease inhibitors were obtained from Solaibao Biotechnology, Co. Ltd. (Beijing, China). phosphorylated AKT (P-Akt) /Akt/Bax/Bcl-2 rabbit antibodies were purchased from ABclonal Technology Co., Ltd. (Wuhan, China). Goat anti-rabbit secondary antibodies were purchased from Abcom (Cambridge, MA, USA). Acetonitrile and ammonium acetate were purchased from Tianjin Kemiou Chemical Reagent Co. Ltd. (Tianjin, China).

### 2.2. Animals

The animal study was approved by the Tianjin University of Traditional Chinese Medicine Use Committee (approval number TCM-LACE2022226). Male eight-week-old C57BL/6 mice (weighing 23 ± 0.2 g) were purchased from Beijing Huafukang Biotechnology Co. Ltd. (Beijing, China) and housed at room temperature (RT; 22 ± 2 °C) under a standard 12h light/dark cycle with free access to food and water. The mice were randomly assigned to three groups: the control group (Control; $n$ = 13), the rotenone group (Model; $n$ = 13), the rotenone+ DZF group (Model + DZF; $n$ = 13).

### 2.3. Experimental design

To establish a suitable PD model, 10 mg/kg of rotenone was suspended in 0.5% carboxymethyl cellulose. Each mouse in the rotenone and rotenone + DZF groups was administrated orally once a day for 3 months. *Dried Eucommia ulmoides*, *Dendrobium*, *Rehmanniae Radix*, and *Dried Ginger* at a ratio of 200:2:3:3 by weight, were refluxed twice in 75% ethanol (reflux for 2 hours each time), and the refluxed supernatant was collected, filtered and concentrated to obtain Duzhong Fang extract (about 11% yield). From the third month, Rotenone + DZF were orally administered 20g/kg/day of DZF for 5 months. The dosages of DZF and rotenone were selected based on previous research (*9*).

2.4. Behavioral tests

2.4.1. Pole test

Place the mouse on top of the vertical pole. Record the time it began to crawl down to the landing of the hind limbs. If the mouse pauses or crawls in the middle, it will be re-measured. If it exceeds 60 s, it will be recorded as 60 s. 3 days before the formal experiment, the mice began to conduct behavioral training once a day for 3 consecutive days. One hour after the last dose, the test was formally started and repeated 3 times. The result of the experiment was the average time.

2.4.2. Rotarod test

The mouse was placed on the rotating rod and moved with the rotating rod at a speed of 25 r/min, and the time of the mouse falling was recorded. If the time exceeds 300 s, record 300 s. The mice were trained before the formal experiment. The formal experiment was repeated 3 times with an interval of 5 min each time, and the average value was calculated.

2.4.3. Grip strength

The mouse was placed on the gripper with its body perpendicular to the metal rod on the dynamometer, and the tail was pulled back at a constant speed to measure the grip. Record the reading and repeat three times to calculate the average value.

2.5. Immunohistochemical staining

The mice were deeply anesthetized and sacrificed by cardiac perfusion with normal saline and 4% paraformaldehyde successively. The whole brain was taken out and fixed with paraformaldehyde and immersed in 30% sucrose for storage at 4°C before sectioning. The brain was sliced into 10 μm coronal sections by frozen sectioning and the sections containing Scripted Non-Playable Character (SNpc) were collected.

Heat-citrate pretreatment was used for antigen retrieval. The tissue sections were treated with 0.25% Triton-100 X to make the tissues permeable, and goat serum was added to block. After blocking, microglia and neurons were detected by immunohistochemical staining with TH antibody, Iba-1 antibody and Neu-N antibody, respectively. Samples were incubated at 4°C overnight with primary antibodies diluted in Bovine Serum Albumin (BSA): anti-TH (1:400), anti-Iba-1(1:400), and anti-Neu-N (1:400). Then the corresponding secondary antibodies, tagged goat anti-rabbit (1:500) were used. Microglia and neuron analysis were captured using a fluorescence microscope.

2.6. Morris water-maze (MWM) test

Spatial learning and memory abilities of were tested with the MWM. The test was carried out using the black circle pool filled with water (22 ± 1°C). The pool was artificially divided into four quadrants (*i.e.*, N, E, S, and W), and the escape platform was located water surface in the quadrant. The mice were released at the farthest position from where the platform had been, if an animal did not find the platform within 60 s of placement in the quadrant, they were guided to the platform and kept there for 30 s. The task consisted of a 6-day acquisition phase with four trials/day. The performances were continuously monitored using an automated tracking system (Noldus Ethovision XT System, the Netherlands). The escape latency to find the platform and the total distance traveled during acquisition were recorded and analyzed.

On the 6th day, spatial memory function was evaluated, the platform was removed and animals were allowed to swim freely for 60 s. The time spent in the target quadrant and the average swim speed were recorded and analyzed.

2.7. The metabolomic assay and data analysis

After a 5-month intervention of DZF, blood was taken by removing the eyeball after fasting for 8 h, centrifuged at 3,000 r/min for 10 min at 4℃ to obtain serum. Chromatographic separations were performed using the ultra-high performance liquid chromatography with quadrupole time-of-flight mass spectrometry (UHPLC-Q-TOF/MS) system. The samples were collected on Agilent 1290 Infinity LC. The mobile phase consisted of solvent A (water + 25 mM ammonium acetate + 25 mM ammonia water) and solvent B (acetonitrile), the gradient elution conditions were set as follows: 0-0.5 min, 95% phase B; 0.5-7 min, 95%-65% phase B; 7-8 min, 65%-40% phase B; 8-9 min, 40% phase B, 9-9.1 min, 40%-95% phase B; 9.1-12 min, 95% phase B; 12.1 min, stop. The triple TOF Mass Spectrometer Detector (AB SCIEX) was used to collect data. The ESI source operation parameters were as follows: ion source temperature, 600°C; ion spray voltage, 5500 V; curtain gas, 30.0 psi; One primary mass spectrometry scan range was mass-to-charge ratio 60 to 1,000 Da. The secondary mass spectrometry scan range was a mass-to-charge ratio of 25 to 1,000 Da. QC samples were inserted into the analytical sequence to evaluate the stability of the analytical system during running samples.

The total ion current data were collected by UHPLC-Q-TOF/MS. The data matrix of the sample name and peak intensity was processed by peak matching, peak alignment, control processing, and multivariate statistical analysis. Partial least squares discriminant analysis was used to obtain the score plot by SIMCA. Significant metabolic markers were selected from discriminant analysis and multivariate statistical methods. Variable importance in projection (VIP) values obtained from the orthogonal partial least-squares discriminant analysis

(OPLS-DA) model was used to select variables with the most important impact, and then *t*-tests were performed. The metabolites with VIP > 1 and $P < 0.05$, which is the top 15, were used for pathway enrichment analysis.

2.8. Network target prediction

First of all, compounds in DZF were chosen for the prediction of biological targets using the TCMSP (*http://tcmspw.com/*). Then, these components were put into the SwissTargetPrediction database (*http://www.swisstargetprediction.ch/*) to obtain the Uniprot ID of predicted targets. Next, the biological targets related to PD-CI were selected from the GeneCards (*https://www.genecards.org/*) and OMIM (*https://www.omim.org/*) database. Taking the intersection of the DZF targets and the candidate targets associated with PD-CI as potential therapeutic targets of DZF against PD-CI. The Kyoto Encyclopedia of Genes and Genomes (KEGG) pathway analysis was performed to identify the enriched top ten pathways of potential therapeutic targets based on the KEGG database.

2.9. Western blotting analysis

The hippocampus, cortex and midbrain ($n = 6$ in each group) were lysed with RIPA lysis buffer. Proteins (25 μg per lane) were separated by 10% or 12% sodium dodecyl sulfate-polyacrylamide gel electrophoresis and transferred to the PVDF membrane. Each membrane was blocked in 5% skim milk powder for 1 h at room temperature and then incubated with anti-Akt (1:1,000), anti-p-Akt (1:1,000), anti-Bax (1:1,000), anti-Bcl-2 (1:1,000), anti-tyrosine hydroxylase (1:1,000), at 4°C overnight. The membranes were incubated with goat anti-rabbit IgG or goat anti-mouse IgG (1:1,000) for 1.5h at room temperature. Blots were imaged by the ECL chemiluminescence (Millipore, USA) and a Gel Image System (GE, USA). Band intensities were quantified using Image J software.

2.10. Statistical analysis

SPSS 22.0 software was used for data analysis. Data were expressed as the mean ± standard error of the mean (SEM). Before performing parametric tests, data distributions were tested for normality using the Kolmogorov–Smirnov test. Differences between groups in behavioral tests were analyzed using one-way ANOVA followed by Tukey post-hoc test and $P < 0.05$ is considered statistically significant.

**3. Results**

3.1. DZF improved locomotor dysfunction and TH levels in the substantia nigra of PD mice

To evaluate the potential protective effect of DZF on locomotor dysfunction in Parkinsonian mice, we performed behavioral tests on mice to evaluate their muscle strength, mobility and balance. Through behavioral testing, compared with the control group, rotenone-induced Parkinsonian mice showed locomotor dysfunction, including longer climbing time, shorter falling time of the rotating rod and lower grip value. However, the DZF treatment used could ameliorate this situation. The results are presented in Figures 2A-2C.

To investigate the protective effects of DZF on dopaminergic neurons in the substantia nigra of PD mice, TH was detected by immunohistochemical staining and Western blot analysis. Immunohistochemical staining revealed a significant loss of $TH^+$ dopaminergic neurons in model mice compared to the control and DZF group (Figure 2D). Western blot analysis showed that TH expression in the model was lower compared to control and DZF (Figures 2E-2F), the results above indicate that DZF inhibited the reduction of TH expression and protected dopaminergic neurons in PD mice.

3.2. DZF improved the cognitive impairment of PD mice

The escape latency of each group was longest on day 1. From day 5 to day 6, it was observed that the escape latency was decreased in the control and DZF group compared to the model group (Figure 3A). As shown in Figure 3B, the frequency of crossing the platform and platform retention time on day 6 was decreased in the model group compared to the control group, while the DZF treatment used could ameliorate this situation (Figures 3B-3C). Conversely, the latency to reach the platform and the escape passage was increased in the model group compared to the control group, but this effect is still ameliorated significantly following DZF treatment (Figures 3D-3E). The above results suggested that DZF can improve the cognitive impairment of PD mice.

3.3. DZF inhibited microglial overactivation in the hippocampus and cortex

The overactivation of microglia is closely related to the progression of cognitive impairment is well known (*10*). To determine the effect of DZF on microglial cell activation, immunofluorescent staining for Iba-1 in microglia was performed. As shown in Figure 4A, the microglia from the model group with larger soma and thicker but shorter protrusions. Microglia return to normal morphology after DZF treatment. Compared with the model group, microglia in DZF-treated mice displayed an increased number of branches and branch endpoints in the hippocampus (Figures 4D-4E). Like the hippocampus, DZF also inhibited microglial overactivation in the cortex (Figures 4F-4J).

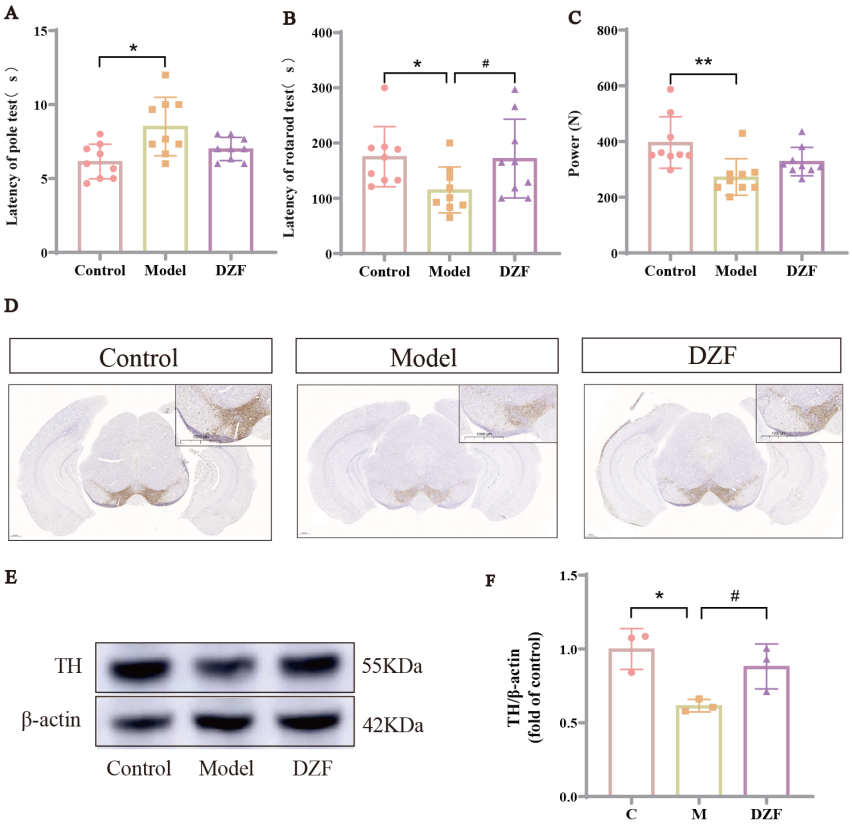


**Figure 2. DZF improved rotenone-induced locomotor activity dysfunction including (A) pole, (B) rotarod, (C) grip, (D) TH level in the substantia nigra by immunohistochemistry, (E) TH protein expression in the substantia nigra, and (F) quantitative results of TH level.** Data represent the means ± SEM ($n$ = 3 per group); Statistics one-way ANOVA; $^{*}P < 0.05$ versus control group; $^{\#}P < 0.05$ versus model group.

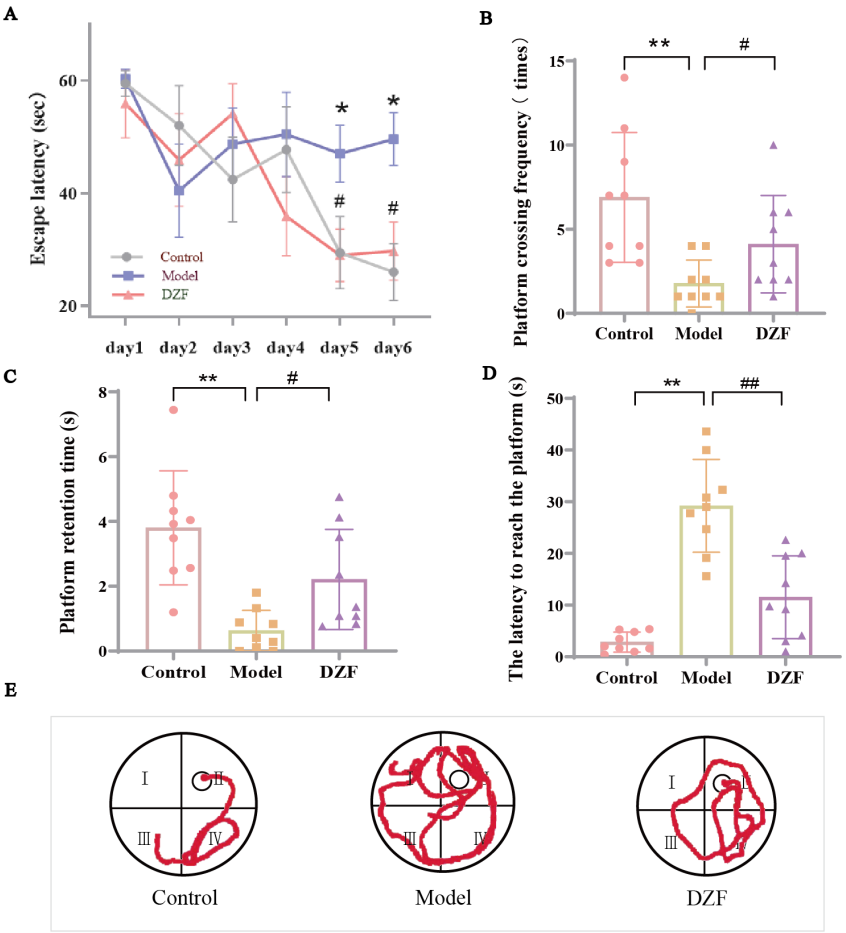


**Figure 3. DZF improved the cognitive impairment of PD mice.** (**A**) Escape latency from day 1 to day 6. (**B**) The platform crossing frequency on day 6. (**C**) The platform retention time on day 6. (**D**) The latency to reach the platform on day 6. (**E**) Escape passage on day 6. Data represent the means ± SEM ($n$ = 9 per group); Statistics one-way ANOVA; $^{*}P < 0.05$ versus control group, $^{**}P < 0.01$ versus control group; $^{\#}P < 0.05$ versus model group, $^{\#\#}P < 0.01$ versus model group.

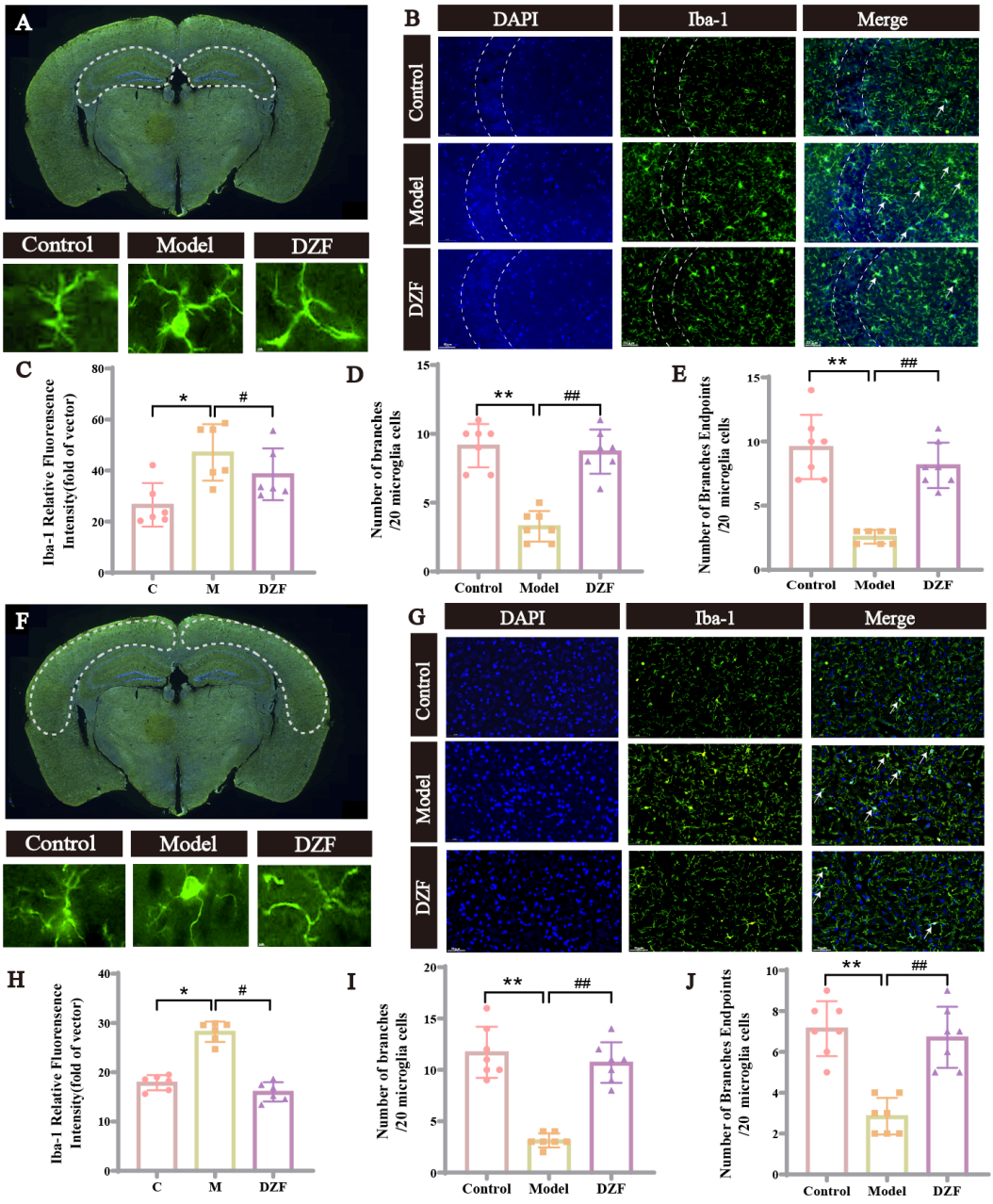


**Figure 4. DZF inhibited microglial overactivation in the hippocampus and cortex.** (**A**) Microglia in the hippocampus. (**B**) Photomicrographs of immunofluorescence staining for microglial cells in the hippocampus. (**C**) Iba-1 relative fluorescence intensity in the hippocampus. (**D**) Average number of branches in the hippocampus. (**E**) Branches endpoints of microglia in the hippocampus. (**F**) Microglia in the cortex. (**G**) Photomicrographs of immunofluorescence staining for microglial cells in the cortex. (**H**) Iba-1 relative fluorescence intensity in the cortex. (**I**) Average number of branches in the cortex. (**J**) Branches endpoints of microglia in the cortex. Six visual fields were randomly selected and 20 cells in each visual field were counted. Data represent the means ± SEM ($n$ = 6 per group); Statistics one-way ANOVA; *$P$ < 0.05 versus control group, **$P$ < 0.01 versus control group; $^{\#}P$ < 0.05 versus model group, $^{\#\#}P$ < 0.01 versus model group.

### 3.4. DZF influences sphingolipid metabolism

The OPLS-DA score plot suggested that the inter-groups were well separated, and the DZF group was closer to the control group than the model group, indicating that DZF had a good therapeutic effect (Figure 5A). The differential metabolites between the control group and the model group as well as between the model group and the DZF group were obtained, we take the intersections of the results and there are 28 differential metabolites were obtained (Figure 5B). A cluster heat plot showed different metabolites and their relative increase or decrease in values among different groups, and after treating with DZF, the levels of the metabolites were close to those in the control group (Figure 5C). In addition, we screened the metabolites with VIP top 15 (Figure 5D), and then searched for these metabolites in the Kyoto encyclopedia of genes and genomes (KEGG) database (*http://www.kegg.com*). Their main metabolic pathways including necroptosis signaling pathway and

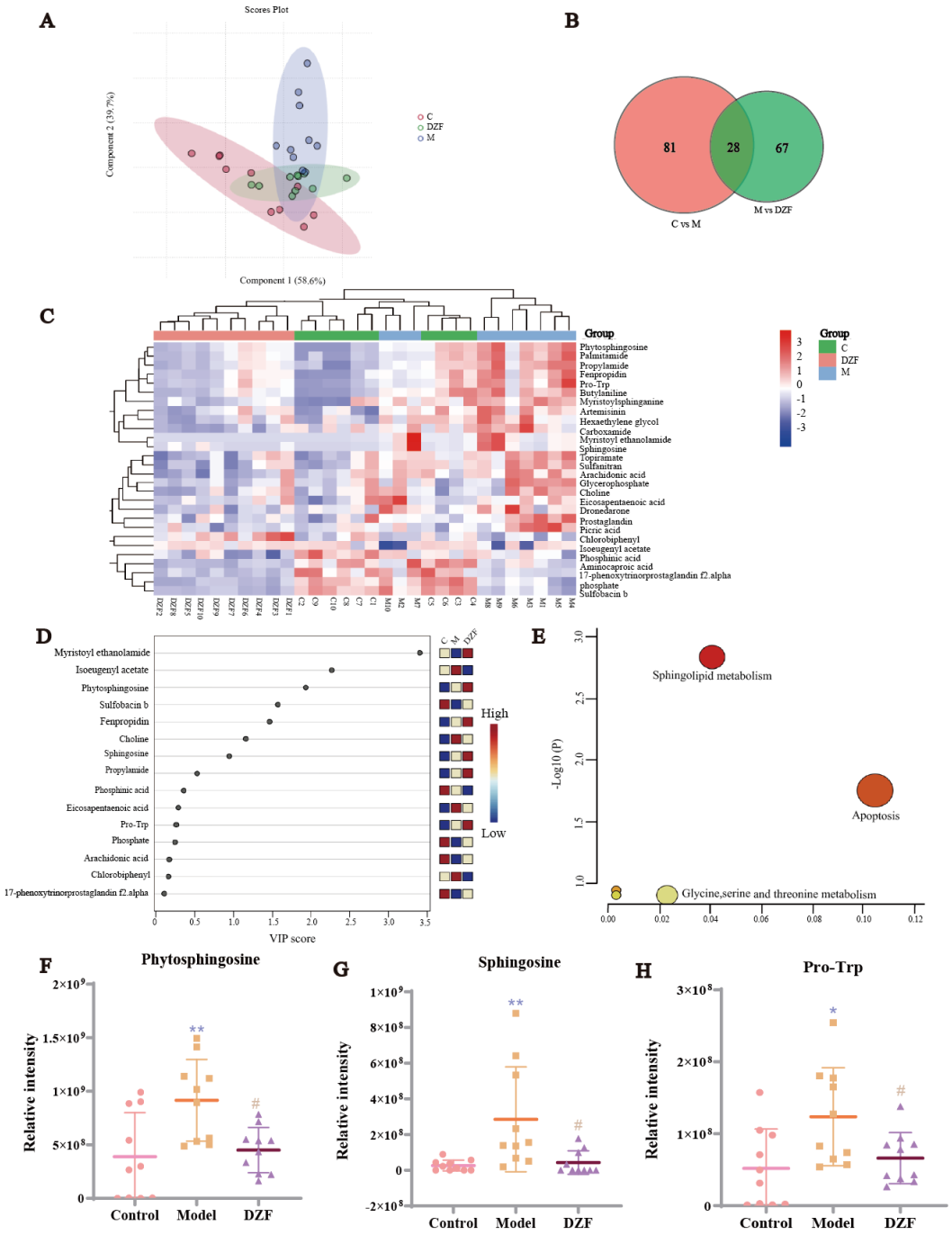


**Figure 5. The effect of DZF on serum metabolites.** (**A**) The OPLS-DA score plot of each group after. (**B**) The differential metabolites intersections among the control group and the model group as well as between the model group and the DZF group. (**C**) The cluster heat plot of each group after treatment. (**D**) The VIP plot of each group after treatment. (**E**) Main metabolic pathway impact analysis. The relative content changes of potential metabolites. (**F**) Phytosphingosine. (**G**) Sphingosine. (**H**) Pro-Trp. Data represent the means ± SEM ($n$ = 10 per group); Statistics one-way ANOVA; $^{*}P < 0.05$ versus control group, $^{**}P < 0.01$ versus control group; $^{\#}P < 0.05$ versus model group.

sphingolipid metabolism signaling pathway (Figure 5E). Finally, by comparing the relative content changes in these differential metabolites in sphingolipid signaling pathway, three potential metabolites were identified (Figures 5F-5H). Therefore, results suggested that DZF can regulate sphingolipid signaling pathway and downregulate the potential metabolites such as phytosphingosine, Pro-Trp and sphingosinne.

### 3.5. DZF treatment suppressed hippocampal and cortex neuronal apoptosis

Active ingredients in DZF with criteria such as oral bioavailability (OB) ≥ 30% and drug-likeness (DL) ≥ 0.18 were selected. We intersected the PD-CI targets with the DZF targets and received 393 common targets (Figure 6A). KEGG pathway enrichment analysis of target genes

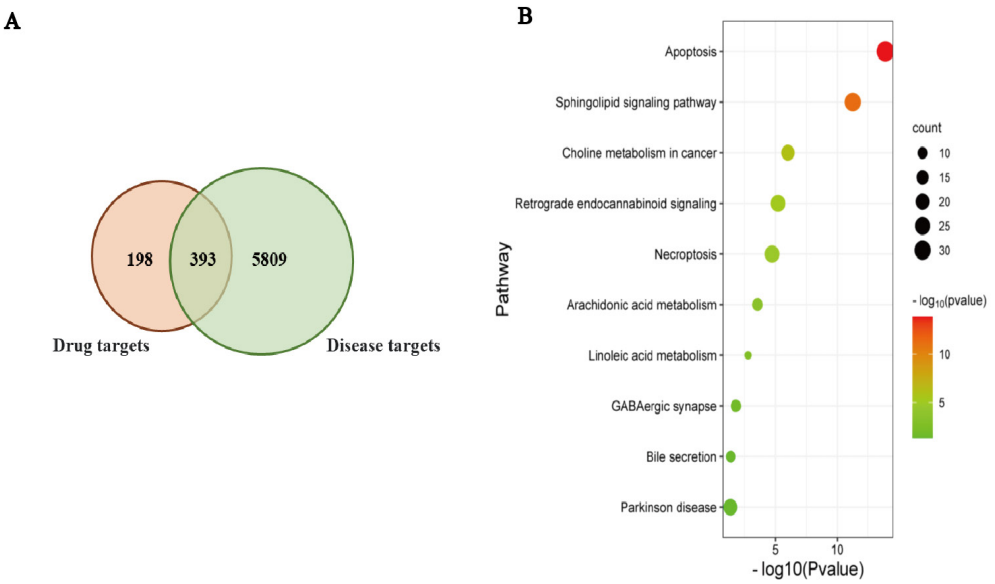


**Figure 6. Potential mechanisms of DZF ameliorating cognitive impairment.** (**A**) The Venn diagram is the intersection of key disease targets and drug targets. (**B**) Enrichment analysis of common targets pathway.

showed that these target genes were enriched in apoptosis (Figure 6B).

To further determine the mechanism of DZF ameliorate cognitive impairment, neuronal apoptosis and the expression of Bax, Bcl-2 and AKT in the hippocampus and cortex regions were examined by immunofluorescence staining and western blot analysis. In the hippocampus, it could be observed that the number of NeuN expressed positive cells was upregulated in the model group compared with the control group (Figures 7A-7B), which were then decreased by DZF treatment compared with the model group. The expression of apoptosis-related proteins Bax proteins was upregulated, while Bcl-2 and p-Akt protein was downregulated in the model group, which was then reversed in mice that received DZF treatment (Figures 7C-7D). It is noteworthy that we also examined neuronal apoptosis and Bax, Bcl-2 and AKT expression in the cortex, the results indicated that protein expression in the cortex and hippocampus showed the same tendencies (Figures 7E-7H). The above results show that DZF treatment attenuated cognitive impairment *via* inhibition of the Bax/Bcl-2-mediated neuronal apoptosis pathway.

## 4. Discussion

Currently, PD-CI treatment is based mainly on AD pharmacotherapy and the first-line drugs include acetylcholinesterase inhibitors, but more than 50% of patients produce serious side effects, such as headaches, nausea, fatigue, anorexia, anxiety, and depression (*11,12*). We hope to screen for more targeted and safe alternatives to treat PD-CI. DZF consists of *Eucommia ulmoides*, *Dendrobium*, *Rehmanniae Radix*, and *Dried Ginger*. This study confirmed that DZF could improve motor deficits and reduce the loss of dopaminergic neurons in PD mice, which was consistent with our previous study. Furthermore, shortened escape latency in a Morris water maze test indicated that DZF improved learning and memory in PD mice. Currently, PD-CI is thought to be associated with excessive activation of microglial cells and apoptosis (*13,14*). It has been reported that over-activated microglia can drive neuroinflammation, release a large number of cytokines and induce neuronal apoptosis (*15*). Over-activated microglia can also enhance autophagy, over-pruning and damage neuronal synapses, leading to cognitive impairment (*16*). Therefore, in this study, immunofluorescence was used to detect microglia and neurons in the hippocampus and cortex. The results showed that the microglia in the hippocampus and cortex of PD mice were over-activated, the cell morphology changed obviously, and the number of neurons decreased significantly. However, DZF could inhibit the activation of microglia and increase the number of neurons. To find out the pharmacological mechanism of DZF in improving cognitive impairment, we further analyzed the serum metabolomics of PD mice, metabolomics results showed that DZF can effectively regulate the pathway metabolites, inhibit phytosphingosine, Pro-Trp and sphingosine levels. In cells, sphingolipid metabolites function as second messengers in signal transduction pathways and regulate cell proliferation, migration and apoptosis (*17*). Furthermore, sphingolipids can affect the cell membrane fluidity and permeability to regulate the balance of the internal and external environments and protect cell stability. Araujo *et al*. reported that sphingolipids can regulate cognitive impairment through the glutamine pathway and sphingolipid metabolic

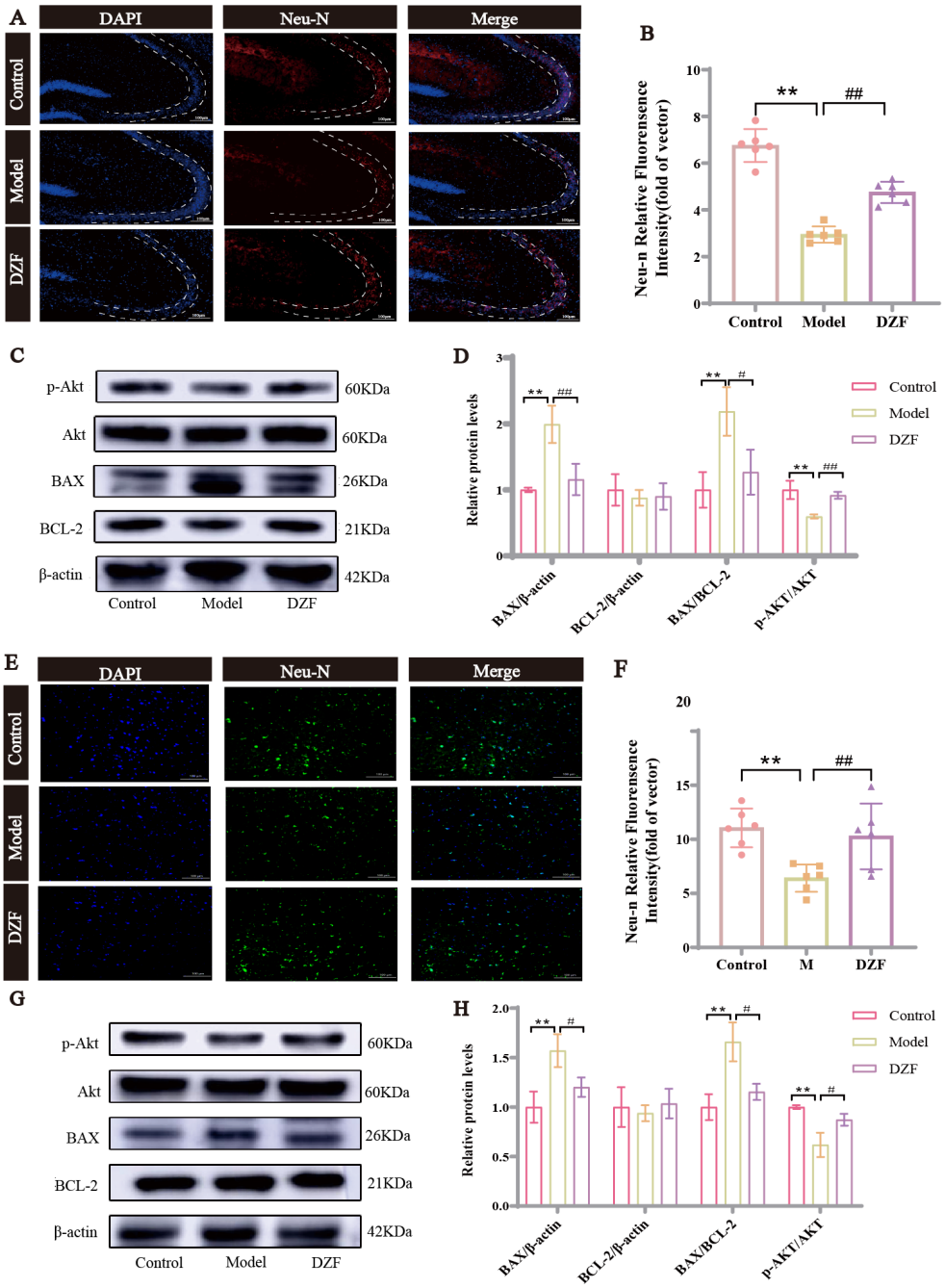


**Figure 7. DZF inhibits apoptosis in neuronal.** (**A**) Staining of Neu-N (red) in the hippocampus. The scale bar is 100μm. (**B**) Neu-N relative fluorescence intensity in the hippocampus ($n$=6 mice per group in Figures A-B). (**C**, **D**) Immunoblotting results show the changes in levels of Bax, Bcl-2 and Akt in the hippocampus ($n$=6 mice per group). (**E**) Staining of Neu-N (green) in the cortex. The scale bar is 100 μm. (**F**) Neu-N relative fluorescence intensity in the cortex ($n$ = 6 mice per group in Figures E-F). (**G**, **H**) Immunoblotting results show the changes in levels of Bax, Bcl-2 and Akt in the cortex ($n$=6 mice per group). Statistics one-way ANOVA; $^{*}P < 0.05$ versus control group, $^{**}P < 0.01$ versus control group; $^{\#}P < 0.05$ versus model group, $^{\#\#}P < 0.01$ versus model group.

pathways (*18*).

In addition to serum metabolomics analysis, we also used network pharmacology to predict the targets of the active ingredients of DZF. A total of 393 targets were obtained by crossing the active ingredients of DZF with PD-CI targets, and the pathway enrichment analysis showed that the apoptosis pathway ranked first. It has been reported that the sphingolipid metabolic pathway can regulate apoptosis, and sphingolipid metabolites can be used as signaling molecules to regulate the activity of apoptosis-related protein kinases (*19*). Phytosphingosine caused the release of proapoptotic factors into the cytoplasm and the expression of apoptosis-related proteins Bax, and Bcl-2 in cells (*20*). Moreover, phytosphingosine decreases phosphorylated Akt to induce apoptosis (*21*). Therefore, we further verified the results of network pharmacology, and the results confirmed that DZF could inhibit the apoptosis-related

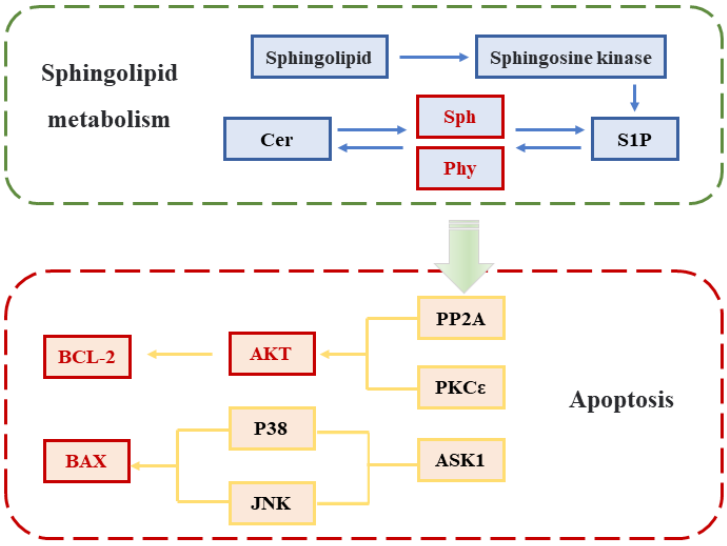


**Figure 8. Possible mechanism of DZF for ameliorating the cognitive impairment in PD mice.** Key steps affected by DZF are highlighted in red circles.

proteins Bax and Bax/Bcl-2, and increase the level of the upstream apoptosis protein p-Akt. In conclusion, our results suggest that DZF could ameliorate PD-CI by regulating the sphingolipid metabolic pathway, inhibiting apoptosis and protecting microglia and neurons. This study provides potential drugs for improving PD-CI and an experimental basis for the clinical application of DZF.

Many of the components in DZF have been shown to inhibit neuroinflammation and apoptosis, which in turn improves cognitive impairment (*22-25*). The mechanisms by which *Dendrobium nobile* Lindl. alkaloid from *Dendrobium* has been reported to improve cognitive dysfunction may be associated with inhibition of neuroinflammation and neuronal apoptosis, activation of autophagy, and enhanced synaptic connections (*26,27*). *Eucommia ulmoides* can downregulate p38/JNK-Fosl2 gene expression to alleviate neuroinflammation and behavioral impairments in PD mice (*28*). *Rehmanniae Radix* inhibits the p38 MAPK pathways and downstream apoptosis-related molecules to alleviate neural cell loss, reduce oxidative stress and promote functional recovery of PD (*29-31*). Our study revealed that the DZF treatment may trigger the sphingolipid metabolism signaling pathway and in turn, affect the cell apoptosis pathway to ameliorate PD-CI. These putative mechanisms are schematically summarised in Figure 8.

## 5. Conclusion

Our study confirmed that DZF ameliorates PD-CI by inhibiting neuronal apoptotic pathway. More specifically, DZF could inhibit neuronal apoptosis linked with Bax/Bcl-2 apoptotic signaling pathways by downregulating the sphingolipid metabolites, including phytosphingosine, sphingosine and Pro-Trp. Taken together, our results provide novel evidences that DZF can be a therapeutic agent for PD-CI.

*Funding*: This work was supported by grants from the National Natural Science Foundation of China (81703827).

*Conflict of Interest*: The authors have no conflicts of interest to disclose.

## References

1. Xu R, Hu X, Jiang X, Zhang Y, Wang J, Zeng X. Longitudinal volume changes of hippocampal subfields and cognitive decline in Parkinson's disease. Quant Imaging Med Surg. 2020; 10:220-232.
2. Fan Y, Li Y, Yang Y, Lin K, Lin Q, Luo S, Zhou X, Lin Q, Zhang F. Chlorogenic acid prevents microglia-induced neuronal apoptosis and oxidative stress under hypoxia-ischemia environment by regulating the MIR497HG/miR-29b-3p/SIRT1 Axis. Dis Markers. 2022; 2022:1194742.
3. Lin WC, Huang YC, Leong CP, Chen MH, Chen HL, Tsai NW, Tso HH, Chen PC, Lu CH. Associations between cognitive functions and physical frailty in patients with Parkinson's disease. Front Aging Neurosci. 2019; 11:283.
4. Benkert J, Hess S, Roy S, *et al*. Cav2.3 channels contribute to dopaminergic neuron loss in a model of Parkinson's disease. Nat Commun. 2019; 10:5094.
5. Li L, Fan S, Zhang W, Li D, Yang Z, Zhuang P, Han J, Guo H, Zhang Y. Duzhong Fang Attenuates the POMC-Derived Neuroinflammation in Parkinsonian Mice. J Inflamm Res. 2021; 14:3261-3276.
6. Lee HS, Kim JM, Lee HL, Go MJ, Lee DY, Kim CW, Kim HJ, Heo HJ. *Eucommia ulmoides* leaves alleviate cognitive dysfunction in dextran sulfate sodium (DSS)-induced colitis mice through regulating JNK/TLR4 signaling pathway. Int J Mol Sci. 2024; 25:4063.
7. Zheng Y, Zhou X, Wang C, *et al*. Effect of dendrobium mixture in alleviating diabetic cognitive impairment associated with regulating gut microbiota. Biomed

Pharmacother. 2022; 149:112891.
8. Su Y, Liu N, Sun R, Ma J, Li Z, Wang P, Ma H, Sun Y, Song J, Zhang Z. Radix Rehmanniae Praeparata (Shu Dihuang) exerts neuroprotective effects on ICV-STZ-induced Alzheimer's disease mice through modulation of INSR/IRS-1/AKT/GSK-3β signaling pathway and intestinal microbiota. Front Pharmacol. 2023; 14:1115387.
9. Wang JP, Sun XJ. Effect of Rehmannia on 6-hydroxydopamine-induced oxidative stress in dopaminergic nerve cells. Zhongguo Lao Nian Xue Za Zhi. 2022; 42:4078-4082. (in Chinese).
10. Cao T, Zhou X, Zheng X, Cui Y, Tsien JZ, Li C, Wang H. Histone deacetylase inhibitor alleviates the neurodegenerative phenotypes and histone dysregulation in presenilins-deficient mice. Front Aging Neurosci. 2018; 10:137.
11. Shen H, Kihara T, Hongo H, Wu X, Kem WR, Shimohama S, Akaike A, Niidome T, Sugimoto H. Neuroprotection by donepezil against glutamate excitotoxicity involves stimulation of alpha7 nicotinic receptors and internalization of NMDA receptors. Br J Pharmacol. 2010; 161:127-139.
12. Yoon SK, Bae KS, Hong DH, Kim SS, Choi YK, Lim HS. Pharmacokinetic evaluation by modeling and simulation analysis of a donepezil patch formulation in healthy male volunteers. Drug Des Devel Ther. 2020; 14:1729-1737.
13. Santisteban MM, Ahmari N, Carvajal JM, Zingler MB, Qi Y, Kim S, Joseph J, Garcia-Pereira F, Johnson RD, Shenoy V, Raizada MK, Zubcevic J. Involvement of bone marrow cells and neuroinflammation in hypertension. Circ Res. 2015; 117:178-191.
14. Cunnane SC, Trushina E, Morland C, *et al*. Brain energy rescue: an emerging therapeutic concept for neurodegenerative disorders of ageing. Nat Rev Drug Discov. 2020; 19:609-633.
15. Subhramanyam CS, Wang C, Hu Q, Dheen ST. Microglia-mediated neuroinflammation in neurodegenerative diseases. Semin Cell Dev Biol. 2019; 94:112-120.
16. Xiong S, Su X, Kang Y, Si J, Wang L, Li X, Ma K. Effect and mechanism of chlorogenic acid on cognitive dysfunction in mice by lipopolysaccharide-induced neuroinflammation. Front Immunol. 2023; 14:1178188.
17. Ahn EH, Yang H, Hsieh CY, Sun W, Chang CC, Schroeder JJ. Evaluation of chemotherapeutic and cancer-protective properties of sphingosine and C2-ceramide in a human breast stem cell derived carcinogenesis model. Int J Oncol. 2019; 54:655-664.
18. Araujo JA, Segarra S, Mendes J, Paradis A, Brooks M, Thevarkunnel S, Milgram NW. Sphingolipids and DHA improve cognitive deficits in aged beagle dogs. Front Vet Sci. 2022; 9:646451.
19. Chipuk JE, McStay GP, Bharti A, Kuwana T, Clarke CJ, Siskind LJ, Obeid LM, Green DR. Sphingolipid metabolism cooperates with BAK and BAX to promote the mitochondrial pathway of apoptosis. Cell. 2012; 148:988-1000.
20. Li J, Wen J, Sun C, Zhou Y, Xu J, MacIsaac HJ, Chang X, Cui Q. Phytosphingosine-induced cell apoptosis *via* a mitochondrially mediated pathway. Toxicology. 2022; 482:153370.
21. Nagahara Y, Shinomiya T, Kuroda S, Kaneko N, Nishio R, Ikekita M. Phytosphingosine induced mitochondria-involved apoptosis. Cancer Sci. 2005; 96:83-92.
22. Caruso G, Godos J, Privitera A, Lanza G, Castellano S, Chillemi A, Bruni O, Ferri R, Caraci F, Grosso G. Phenolic acids and prevention of cognitive decline: Polyphenols with a neuroprotective role in cognitive disorders and Alzheimer's disease. Nutrients. 2022; 14:819.
23. Fan Y, Li M, Wu C, Wu Y, Han J, Wu P, Huang Z, Wang Q, Zhao L, Chen D, Zhu M. Chronic cerebral hypoperfusion aggravates Parkinson's disease dementia-like symptoms and pathology in 6-OHDA-lesioned rat through interfering with sphingolipid metabolism. Oxid Med Cell Longev. 2022; 2022:5392966.
24. Han N, Wen Y, Liu Z, Zhai J, Li S, Yin J. Advances in the roles and mechanisms of lignans against Alzheimer's disease. Front Pharmacol. 2022; 13:960112.
25. Singh SS, Rai SN, Birla H, Zahra W, Rathore AS, Dilnashin H, Singh R, Singh SP. Neuroprotective effect of chlorogenic acid on mitochondrial dysfunction-mediated apoptotic death of DA neurons in a Parkinsonian mouse model. Oxid Med Cell Longev. 2020; 2020:6571484.
26. Li DD, Zheng CQ, Zhang F, Shi JS. Potential neuroprotection by *Dendrobium nobile* Lindl. alkaloid in Alzheimer's disease models. Neural Regen Res. 2022; 17:972-977.
27. He L, Su Q, Bai L, Li M, Liu J, Liu X, Zhang C, Jiang Z, He J, Shi J, Huang S, Guo L. Recent research progress on natural small molecule bibenzyls and its derivatives in Dendrobium species. Eur J Med Chem. 2020; 204:112530.
28. Fan S, Yin Q, Li D, Ma J, Li L, Chai S, Guo H, Yang Z. Anti-neuroinflammatory effects of *Eucommia ulmoides* Oliv. in a Parkinson's mouse model through the regulation of p38/JNK-Fosl2 gene expression. J Ethnopharmacol. 2020; 260:113016.
29. Imafuku F, Miyazaki I, Sun J, Kamimai S, Shimizu T, Toyota T, Okamoto Y, Isooka N, Kikuoka R, Kitamura Y, Asanuma M. Central and enteric neuroprotective effects by *Eucommia ulmoides* extracts on neurodegeneration in rotenone-induced Parkinsonian mouse. Acta Med Okayama. 2022; 76:373-383.
30. Angelopoulou E, Paudel YN, Papageorgiou SG, Piperi C. Elucidating the beneficial effects of ginger (*Zingiber officinale* Roscoe) in Parkinson's disease. ACS Pharmacol Transl Sci. 2022; 5:838-848.
31. Wang Y, Li LL, Shen Q, Guo MQ, Liu X, Guo H. Duzhong formula improves the intestinal microenvironment of Parkinson's mice. Tianjin Zhong Yi Yao Da Xue Xue Bao. 2023; 42:463-469. (in Chinese)

Received May 22, 2024; Revised June 20, 2024; Accepted June 23, 2024.

[§]These authors contributed equally to this work.
**Address correspondence to:*
Weihong Yang and Hong Guo, State Key Laboratory of Component-based Chinese Medicine, Tianjin University of Traditional Chinese Medicine, Tianjin, 301617, China.
E-mail: ouyang8463@126.com (WY) and cacti1983@163.com (HG)

Released online in J-STAGE as advance publication July 18, 2024.